Avicenna Journal of Phytomedicine (AJP)

Original Research Article

Multi-target healing mechanisms of *Hippobroma longiflora* for diabetic wounds: A comprehensive network pharmacology study, molecular docking, and experimental insights

Happy Elda Murdiana[1,2], Retno Murwanti[3], Hernawan Hernawan[4], Nanang Fakhrudin[5,6], Zullies Ikawati[3,*]

[1]*Doctorate Program of Pharmacy, Faculty of Pharmacy, Universitas Gadjah Mada, Sekip Utara, Yogyakarta, Indonesia*
[2]*Department of Pharmacology and Clinical Pharmacy, Faculty of Pharmacy, Universitas Kristen Immanuel, Yogyakarta, Indonesia*
[3]*Department of Pharmacology and Clinical Pharmacy, Faculty of Pharmacy, Universitas Gadjah Mada, Sekip Utara, Yogyakarta, Indonesia*
[4]*Research Center for Food Technology and Processing, National Research and Innovation Agency, Playen, Gunungkidul, Yogyakarta, Indonesia*
[5]*Department of Pharmaceutical Biology, Faculty of Pharmacy, Universitas Gadjah Mada, Sekip Utara, Yogyakarta, Indonesia*
[6]*Medicinal Plants and Natural Products Research Center, Faculty of Pharmacy, Universitas Gadjah Mada, Sekip Utara, Yogyakarta, Indonesia*

Article history:
Received: Apr 28, 2025
Received in revised form: Jul 03, 2025
Accepted: Aug 06, 2025
Epub ahead of print

**** Corresponding Author:***
Tel: +62815 685 4012
Fax: +62 0274-552956
zullies_ikawati@ugm.ac.id

Keywords:
Diabetic wound healing
Herbal medicine
Network pharmacology
AKT1
TNF-α
HIF-1α

Abstract

Objective: This research investigated the multi-target mechanisms of *Hippobroma longiflora* (HL) in promoting diabetic wound healing using an integrated approach involving network pharmacology, molecular docking, and both in vitro and in vivo evaluations.

Materials and Methods: The bioactive compounds of HL leaves' 70% ethanol extract were detected using liquid chromatography–high-resolution mass spectrometry (LC-HRMS), and potential targets were predicted via the SwissTargetPrediction. Gene ontology (GO) and Kyoto encyclopedia of genes and genomes (KEGG) pathway enrichment analyses were conducted using DAVID. Molecular docking was predicted using MOE version 2015.10. *In vitro* assays using HaCaT cells evaluated proliferation and Tumor Necrosis Factor-alpha (TNF-α) levels via ELISA. *In vivo* measurement in diabetic rats induced by streptozotocin (n = 9 per group), with histopathological analysis conducted on days 7, 14, and 21.

Results: HL extract exhibited anti-inflammatory and pro-proliferative effects, primarily mediated by syringic acid (P41) and vanillactic acid (P43). These compounds upregulated AKT1, MAPK3, and HIF-1α. HL treatment significantly enhanced HaCaT cell proliferation ($p < 0.0001$) and reduced TNF-α level at 31.25 ppm ($p < 0.05$). *In vivo*, HL treatment decreased inflammatory cell infiltration from day 7, with significant tissue regeneration observed by day 14 ($p < 0.01$) relative to base control.

Conclusion: HL and its bioactive constituents demonstrate promising potential for diabetic wound healing by modulating inflammatory mediators (TNF-α) and enhancing key regenerative pathways (AKT1, MAPK3, and HIF-1α).

Please cite this paper as:
Murdiana H.E., Murwanti R, Hernawan H, Fakhrudin N, Ikawati Z. Multi-target healing mechanisms of *Hippobroma longiflora* for diabetic wounds: A comprehensive network pharmacology study, molecular docking, and experimental insights. Avicenna J Phytomed, 2025. Epub ahead of print.

Introduction

Diabetes mellitus is a persistent metabolic disorder marked by disrupted insulin production or utilization (WHO 2016). Among its complications, diabetic foot ulcers (DFUs) pose a significant burden, resulting in a decline in quality of life, elevated risk of infection, and potential limb amputation (Burgess et al. 2021). DFUs result from peripheral neuropathy, vascular impairment, and altered immune responses that delay tissue repair (Davis et al. 2018; Qaseem et al. 2017). If not properly managed, they can develop into gangrene, sepsis, or death (Falanga 2005).

Persistent hyperglycemia contributes to wound chronicity by promoting advanced glycation end-product (AGE) formation, reactive oxygen species (ROS) accumulation, nitric oxide depletion, and sustained inflammation (Liu et al. 2021; Suryavanshi and Kulkarni 2017). These conditions disrupt fibroblast and keratinocyte function, impair angiogenesis, reduce growth factor expression, and deregulate extracellular matrix (ECM) remodeling through matrix metalloproteinases (MMPs) (Deng et al. 2023; Zheng et al. 2023). Elevated interleukin-1β (IL-1β) and tumor necrosis factor-alpha (TNF-α) cytokines perpetuate inflammation. Inhibiting IL-1β promotes healing (Davis et al. 2018), and AGEs stimulate TNF-α production via macrophage activation (den Dekker et al. 2020; Dong et al. 2016). Additionally, MAPK3 is essential for regulating cellular proliferation and regeneration (Wang et al. 2022).

Although therapeutic modalities such as growth factors, oxygen therapy, platelet-rich plasma, and stem cells have been explored, they remain costly, inconsistently effective, and less accessible in resource-limited settings (Murdiana et al. 2024; Zheng et al. 2023). Hyperbaric oxygen therapy may even exacerbate Reactive oxygen species (ROS)/ Reactive nitrogen species (RNS) generation, causing oxidative tissue damage (Raja et al. 2023; Růžička et al. 2021). Prolonged antibiotic use risks antimicrobial resistance, and evidence supporting pharmacological agents like vildagliptin or phenytoin in DFU healing remains weak (Spampinato et al. 2020).

Herbal medicines offer affordable, multi-target, and safer alternatives. *Hippobroma longiflora* (HL), locally known as "kitolod," with the English “Star of Bethlehem or Madam Fate”, is traditionally used in Indonesia and Central America for treating inflammation, wounds, and toothache (Heyne 1987). Ethnopharmacological records such as *Serat Centhini* and *Usada Buddha Kecapi* document its therapeutic use. Phytochemically, HL contains lobeline (alkaloid), flavonoids, and phenolic acid compounds with known anti-inflammatory, antioxidant, and tissue repair agents (Amrati et al. 2023; Chanu et al. 2023; Kesting et al. 2009). However, scientific validation of HL wound-healing effects, especially in diabetic contexts, and its multi-target molecular mechanism remains unexplored.

Despite its ethnomedical relevance, no prior study has systematically elucidated HL molecular mechanisms in diabetic wound healing using integrative tools. To address this gap, we hypothesized that HL promotes wound repair through multi-target modulation of key inflammatory and regenerative pathways. This study aimed to investigate HL therapeutic potential using Liquid Chromatography–High-Resolution Mass Spectrometry (LC-HRMS)-based phytochemical profiling, network pharmacology, molecular docking, and both *in vitro* (HaCaT proliferation, and TNF-α ELISA) and *in vivo* (streptozotocin-induced diabetic rat model) validation. The findings are expected to provide mechanistic insights and support HL development as an accessible botanical therapy for diabetic wounds.

Materials and Methods

Plant material and extraction

Leaves of *Hippobroma longiflora* (L.) *G. Don* was collected from rocky areas around the Mataram ditch, Sleman, Yogyakarta, Indonesia, and authenticated at the Plant Systematics Laboratory, Faculty of Biology, Universitas Gadjah Mada. A voucher specimen was deposited under the identification number 0394/S.Tb./VIII/2023. Two hundred grams of dried leaves were extracted by maceration in 2,000 ml of 70% ethanol, and concentrated using a rotary evaporator (at 40°C). Ethanol was chosen for its effectiveness in extracting polar and semi-polar bioactive compounds while maintaining stability. The resulting crude extract was stored for further analysis. For *in vitro* assays, the HL extract was solubilized in dimethyl sulfoxide (DMSO) to a concentration of 10 mg/50 µl. *In vivo* gel formulations containing 30%, 40%, and 50% extract were prepared using 1% hydroxypropyl methylcellulose (HPMC) as the base.

LC-HRMS analysis and compound target prediction

LC-HRMS analysis was conducted using a Thermo Scientific Vanquish UHPLC system coupled with a Q-Exactive Orbitrap HRMS and an Acclaim™ VANQUISH™ C18 column. The mobile phase was composed of water (0.1% formic acid) and methanol (0.1% formic acid) (Merck). A 10 µl sample was injected and eluted at 0.30 mL/min, with a gradient from 5% to 90% methanol over 20 min, followed by 5 min at 95% aqueous phase. Mass spectrometry parameters included sheath, auxiliary, and sweep gas flow rates of 32, 8, and 4 arbitrary units, respectively. Compounds were identified using Compound Discoverer 3.2 software (Ahda et al. 2023) by comparing MS/MS fragmentation patterns with mzCloud database references, along with retention times and calculated molecular weight. For provisional identification, a matching score of at least 85% was required. Identified bioactive compounds, including polyphenols, flavonoids, and alkaloids, were used for target prediction. The 3D structures were retrieved from the PubChem database (http://pubchem.ncbi.nlm.nih.gov/), and canonical SMILES (Simplified Molecular Input Line Entry System) strings were submitted to the SwissTargetPrediction platform (http://swisstargetprediction.ch/index.php). The organism filter was set to "*Homo sapiens"*, and only targets with non-zero probability scores were included for downstream analysis.

Network pharmacology and bioinformatics analysis

Targets associated with diabetic wounds were extracted from the GeneCards (https://www.genecards.org) and DisGeNET (https://www.disgenet.org) databases. Venn diagram analysis (InteractiveVenn) (http://www.interactivenn.net/) was used to identify the overlapped target between the bioactive compounds and genes linked to diabetic wounds and then standardized via the UniProt database (https://www.uniprot.org), with the organism filter set to *Homo sapiens*, resulting in a refined list of human genes implicated in diabetic wound pathology.

Protein-protein interaction (PPI) networks were constructed by the STRING database (Search Tool for the Retrieval of Interacting Genes/Proteins; https://string-db.org) and visualized in Cytoscape software v3.10. Critical proteins were identified using the CytoHubba plugin based on degree centrality, with the top five-ranked proteins prioritized due to their relevance in diabetic wound healing.

Gene ontology (GO) and Kyoto encyclopedia of genes and genomes (KEGG) enrichment studies were performed utilizing the database for annotation, visualization, and integrated discovery (DAVID) Bioinformatics Resources (http://david.ncifcrf.gov/), with *Homo sapiens* as the reference genome. Enriched biological processes and pathways

were visualized via Bioinformatics.com.cn to elucidate the functional significance of the target genes (http://bioinformatics.com.cn).

Molecular docking

The three-dimensional (3D) structures of the hub proteins AKT1, MAPK3, and HIF-1α were retrieved from the RCSB Protein Data Bank (https://www.rcsb.org/). Molecular docking analysis was performed using Molecular Operating Environment (MOE) software (v 2015.10), licensed to the Faculty of Pharmacy, Universitas Gadjah Mada. Binding energies below −5.0 kcal/mol were considered indicative of strong ligand–protein interactions (Fu et al. 2022).

HaCaT cell culture and proliferation assay

HaCaT cells were grown in Dulbecco's Modified Eagle Medium (DMEM) enriched with 10% fetal bovine serum (FBS) and 1% antimycotic solution, maintained at 37°C in a humidified 5% CO_2 incubator.

For the proliferation assay, cells were seeded in 96-well plates (1×10^4 cells/cm²) and allowed to grow until the confluence exceeded 90%. After 24 hours of exposure to HL extract or lobeline, the MTT assay (3-(4,5-dimethylthiazol-2-yl)-2,5-diphenyltetrazolium bromide; Sigma-Aldrich) was used to evaluate the cell proliferation; the assay measures mitochondrial activity through conversion of MTT to insoluble formazan. The reaction was stopped with 10% sodium dodecyl sulphate (SDS) in 0.01 N hydrochloric acid (HCl) (Sigma-Aldrich), and absorbance was measured at 570–595 nm utilizing a microplate reader (iMark, Bio-Rad, USA).

TNF-α expression (ELISA)

HaCaT cells were seeded in six-well plates (7×10^5 cells/well in 1,000 µl) of medium and cultured to > 90% confluence. To mimic diabetic conditions, cells were treated overnight with a high-glucose (HG) medium containing 9.0 ppm glucose. HL leaf extract or lobeline was then added, followed by a 6-hr incubation at 37°C in a 5% CO_2 humidified incubator.

Supernatants were obtained and stored at -80°C for the measurement of TNF-α using an ELISA kit (ABclonal®). The normal glucose (NG) control group received 0.9 ppm glucose medium (Chumpolphant et al. 2022). The experiment was performed according to standard protocols, and optical density (OD) was quantified at 450 nm utilizing a microplate reader (Bio-Rad, IndiaMART).

***In vivo* wound healing study**

Male Wistar rats (*Rattus norvegicus*) weighing 180–250 g and aged 8–10 weeks were maintained under standard laboratory conditions (12-hr light/dark cycle at 25°C) with free access to Rad Bio rodent feed and water. All *in vivo* and *in vitro* procedures were ethically approved (No. KE/FK/1490/EC/2023) by the Ethical Clearance Committee of the Faculty of Medicine, Public Health, and Nursing, Universitas Gadjah Mada, Yogyakarta, Indonesia.

Diabetes was produced using a single intraperitoneal administration of streptozotocin (STZ; 45 mg/kg body weight in citrate buffer, pH 4.5). Rats exhibiting fasting blood glucose levels over 200 mg/dl (via eye vein sampling) were considered diabetic (Furman 2021).

Forty-five diabetic rats were assigned randomly to five groups (n = 9): drug control (Mupirocin®), base control (1% HPMC), and HL-treated groups (30%, 40%, and 50% extract gels: K1, K2, and K3, respectively). Anesthesia was induced using a ketamine–xylazine–saline mixture (6.0 ml ketamine 100 mg/ml + 3.75 ml xylazine 20 mg/ml + 29.25 ml 0.9% NaCl). Full-thickness excisional wounds, measuring 8 mm in diameter, were generated on the dorsal skin utilizing a biopsy punch.

Topical treatments were applied daily. Rats were euthanized on days 7, 14, and 21, and wound tissues were obtained for

histological examination utilizing hematoxylin and eosin (H&E) staining.

Histopathology (hematoxylin-eosin staining)

Wound tissues were preserved in 4% paraformaldehyde for 24 hr, thereafter washed, dried, and embedded in paraffin. Sections (4 µm thick) were produced with a microtome (Accu-Cut® SRM, Japan), stretched in 37°C water, mounted, and incubated overnight at 37°C. Slides underwent dewaxing with xylene, rehydrated through a graded ethanol series, and stained with H&E.

Inflammatory cells were assessed using a phase-contrast camera (OptiLab Advance) under light microscopy (Leica 435772, Germany) at 400X magnification. For each sample, five non-overlapping random high-power fields (HPFs) were examined. Image samples were converted to 8-bit grayscale, and a uniform threshold was applied to isolated inflammatory cells. Labeled nuclei were identified automatically using the Analyze Particles function in ImageJ software, based on size and shape parameters.

Statistical analysis

Data were analyzed using GraphPad Prism v8.4.0 (671) (GraphPad Software, San Diego, CA). The Shapiro–Wilk test was performed to assess the normality of data distribution. All results are presented as mean ± standard deviation (SD). Group comparisons were made using one-way ANOVA for TNF-α ELISA data and two-way ANOVA for inflammatory cell counts, followed by Tukey's multiple comparisons test. ANOVA results are reported as F-statistics with corresponding degrees of freedom and p-values. Statistical significance was defined as less than 0.05.

Results

Determination of *H. longiflora* (HL) leaf

The leaf sample used in this study was confirmed as *H. longiflora* (L.) G, with the number 0394/S.Tb./VIII/2023. This species belongs to the Campanulaceae family and is registered under the name *Hippobroma longiflora* (urn:lsid:ipni.org:names:1133957-2).

Identification of HL bioactive compounds via HRMS and compound target prediction

Based on HRMS results, 10 flavonoids, 55 phenolics, and 3 biomarker alkaloids were selected for protein target prediction. Target analysis revealed that the flavonoids interact with 499 proteins, phenolics with 2,593 proteins, and alkaloids with 205 proteins. After removing duplicates, a total of 775 unique target proteins were identified as being influenced by HL compounds. A list of selected active compounds, along with their retention times and abundances, is provided in Supplementary 1. Representative chromatographic peaks of HL compounds are illustrated in Figure 1.

Network of hub protein-protein interaction and bioinformatics analysis

After removing duplicates from 130 GeneCards and 71 DisGeNET entries, 120 diabetic wound-related targets were identified. These were intersected with HL compound targets, yielding 33 overlapping proteins, suggesting a strong mechanistic association with diabetic wound healing (Figure 2A). Of these, 32 human proteins were confirmed using the UniProt database (*Homo sapiens* filter) (Table 1).

Protein–protein interaction (PPI) network of the 32 targets was established via STRING, revealing 230 interactions, an average node degree of 14.4, and a clustering coefficient of 0.763. The network exhibited high interconnectivity ($p<1.0e-16$), indicating potential functional relevance (Figure 2B).

Based on degree centrality, the CytoHubba plug-in Cytoscape, the top hub proteins were AKT1, MAPK3, and HIF-1α, which are key regulators of angiogenesis and cellular proliferation thus were selected for molecular docking.

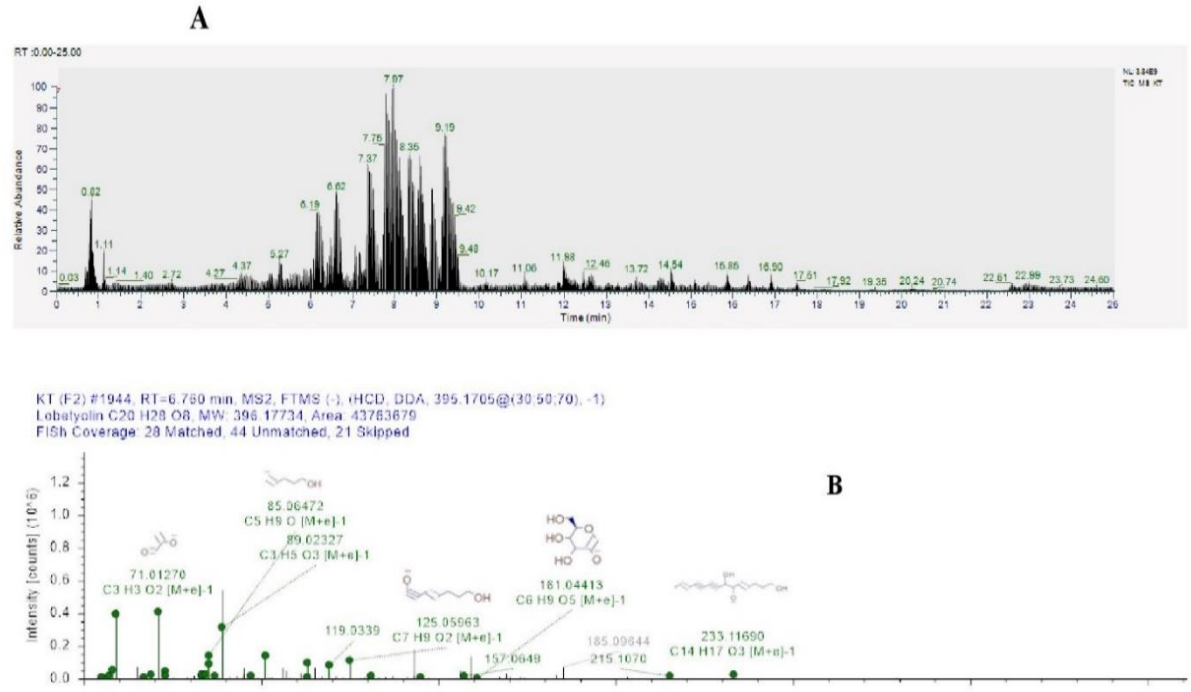

Figure 1. HRMS peaks of *Hippobroma longiflora* extract. (A) shows the untargeted active compounds of HL extract identified by LC-HRMS. (B) displays lobetyolin, a targeted compound and one of HL's biomarkers.

Table 1. Proteins that influence diabetic wounds based on the degree and closeness

Display name	Description	Degree	Closeness centrality
AKT1	RAC-alpha serine/threonine-protein kinase	30	0.968
TNF	Tumor necrosis factor, membrane form	27	0.885
IL1B	Interleukin-1 beta	24	0.815
MAPK3	Mitogen-activated protein kinase 3	23	0.794
HIF1A	Hypoxia-inducible factor 1-alpha	23	0.794
MMP9	Matrix metalloproteinase-9	22	0.775
TLR4	Toll-like receptor 4	22	0.775
KDR	Vascular endothelial growth factor receptor 2	21	0.756
PPARG	Peroxisome proliferator-activated receptor gamma	20	0.738
CXCR4	C-X-C chemokine receptor type 4	19	0.720
MAPK1	Mitogen-activated protein kinase 1	18	0.704
PIK3CA	Phosphatidylinositol 4,5-bisphosphate 3-kinase catalytic subunit alpha isoform	17	0.673
MAPK14	Mitogen-activated protein kinase 14	17	0.688
NOS3	Nitric oxide synthase, endothelial	15	0.659
NFE2L2	Nuclear factor erythroid 2-related factor 2	14	0.645
ESR2	Estrogen receptor beta	14	0.645
PIK3CG	Phosphatidylinositol 4,5-bisphosphate 3-kinase catalytic subunit gamma isoform	13	0.632
MDM2	E3 ubiquitin-protein ligase Mdm2	13	0.632
NOS2	Nitric oxide synthase, inducible	11	0.607
TLR9	Toll-like receptor 9	11	0.607
SELL	L-selectin	10	0.596
PIK3CB	Phosphatidylinositol 4,5-bisphosphate 3-kinase catalytic subunit beta isoform	10	0.584
MMP1	Matrix metalloproteinase-1	9	0.584
PIK3CD	Phosphatidylinositol 4,5-bisphosphate 3-kinase catalytic subunit delta isoform	9	0.584
PTPN1	Tyrosine-protein phosphatase non-receptor type 1	8	0.574
PGF	Placenta growth factor	8	0.574
MME	Neprilysin	8	0.574
SLC5A2	Sodium/glucose cotransporter 2	6	0.553
AURKA	Aurora kinase A	6	0.553
CDC25C	M-phase inducer phosphatase 3	6	0.543
MMP8	Neutrophil collagenase	4	0.500
EGLN1	Egl nine homolog 1	2	0.508

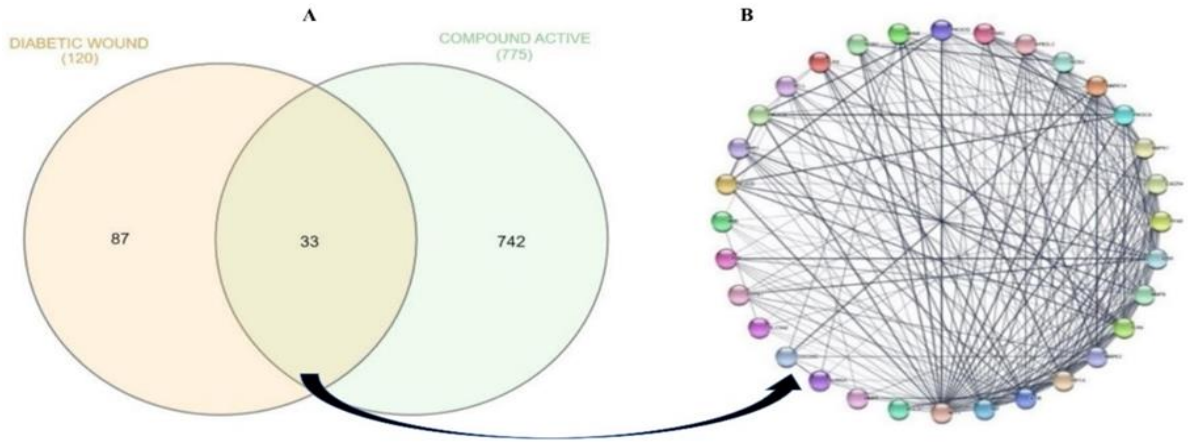

Figure 2. Protein-protein interactions between diabetic wound targets and *Hippobroma longiflora* (HL) compounds. (A) presents a Venn diagram showing the overlap between HL-targeted proteins and diabetic wound-related proteins. (B) illustrates the interaction network among the overlapping proteins.

Gene Ontology (GO) analysis revealed 288 enriched biological processes (BP), 31 cellular components (CC), and 47 molecular functions (MF), with the top 10 term from each category, ranked by p-value, enrichment score, gene count, and rich factor (%), are shown in Figure 3A.

KEGG pathway analysis identified 139 significant pathways, with the top 15 displayed in Figure 3B, ranked by $\log_{10}$(p-value), enrichment score, and gene count. Noteworthy pathways included the HIF-1 signaling, lipid metabolism, atherosclerosis, and cancer-related pathways, reflecting HL potential to modulate critical mechanisms in diabetic wound healing.

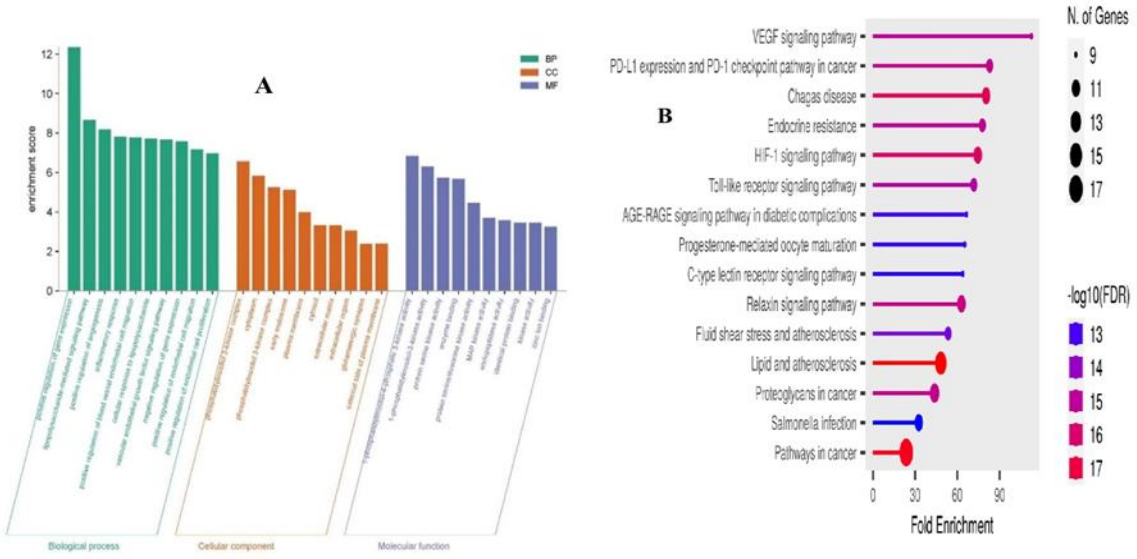

Figure 3. GO and KEGG pathway analysis of *Hippobroma longiflora* in diabetic wound healing. (A) shows GO enrichment results of HL-related genes, categorized into biological processes (green), cellular components (orange), and molecular functions (blue). The top 10 terms in each category are ranked by p-value, enrichment score, gene count, and rich factor (%). (B) displays the KEGG pathway analysis, highlighting key signaling pathways regulated by HL in diabetic wound healing. Dot color and size represent p-value, enrichment score, and several related proteins, with larger and redder dots indicating stronger enrichment.

Molecular docking results

Molecular docking revealed that syringic acid (P41) and vanillactic acid (P43) exhibited strong affinities for the three key hub proteins: AKT1, MAPK3, and HIF-1α (Table 2). P41 showed a high binding affinities to AKT1 (−12.2 kcal/mol), MAPK3 (-5.4 kcal/mol), and HIF-1α (−15.6 kcal/mol), while P43 also demonstrated strong interactions with AKT1 (−12.9 kcal/mol), MAPK3 (−6.1 kcal/mol), and HIF-1α (−10.1 kcal/mol). Among the 68 compounds tested, only these two consistently bound all four targets, suggesting broad modulatory effects on proliferation, angiogenesis, and cell signaling relevant to diabetic wound healing. In contrast, conventional drugs showed limited binding to these key proteins. Figure 4 presents both 2D and 3D docking visualizations. These findings warrant further investigation of P41 and P43 in future studies.

Table 1. The binding energy of *Hippobroma longiflora* (HL) extract active ingredient to the critical protein target

Hub protein target	PDB IDs	Active ingredient	Energy binding (kcal/mol)	Residual interaction	Type of interaction	Distance
AKT1	2 UVM	F7	-9.3	O(14)-NZ.LYS(14)	H-acceptor	2.68
		F9	-6.7	O(49)-NE.ARG(86)	H-acceptor	2.93
		M1	-6.4	O(23)-NZ.LYS(14)	H-acceptor	2.99
		M2	-7.0	O(23)-NZ.LYS(14)	H-acceptor	2.92
		M3	-5.5	O(53)-NZ.LYS(14)	H-acceptor	3.02
		P3	-9.6	O(38)-NH1.ARG(23)	H-acceptor	2.93
		P25	-5.1	O(28)-NH1.ARG(86)	H-acceptor	2.91
		P24	-15.6	O(16)-NZ.LYS(14)	H-acceptor	2.83
		P29	-11.3	O(20)-NZ.LYS(14)	H-acceptor	2.87
		P36	-6.5	O(17)-NZ.LYS(14)	H-acceptor	2.99
		P41	-12.2	O(23)-NZ.LYS(14)	H-acceptor	2.81
		P43	-12.9	O(21)-NZ.LYS(14)	H-acceptor	2.85
		P52	-12.6	O(17)-NZ.LYS(14)	H-acceptor	2.86
		vildagliptin	-28.9	O(43)-NZ_LYS(14)	H-acceptor	2.81
		sitagliptin	-34.9	N(41)-NZ_LYS(14)	H-acceptor	2.97
HIF 1A	1 H2N	F1	-6.8	O(70)-NE2.HIS(199)	H-donor	2.99
		F2	-7.5	O(40)-NE2.HIS(279)	H-donor	2.79
		F5	-8.8	O(36)-NZ.LYS(214)	H-acceptor	2.78
		F7	-11.7	O(24)-NE2.HIS(279)	H-donor	2.87
		F9	-5.7	O(68)-NE2.HIS(199)	H-donor	3.02
		P3	-14.5	O(39)-NZ.LYS(214)	H-acceptor	2.87
		P23	-8.8	N(5)-NE.HIS(199)	H-donor	3.16
		P24	-15.3	O(15)-NZ.LYS(214)	H-acceptor	2.82
		P25	-6.4	O(43)-NE2-HIS(279)	H-donor	3.08
		P29	-13.9	O(21)-NZ.LYS(214)	H-acceptor	2.7
		P31	-13.8	O(20)-NZ.LYS(14)	H-acceptor	2.77
		P38	-5.3	O(37)-NE2.HIS(199)	H-donor	3.09
		P41	-15.6	O(23)-NZ.LYS(14)	H-acceptor	2.68
		P43	-10.1	O(25)-NE2.HIS(199)	H-donor	2.85
		P52	-15.5	O(17)-NZ.LYS(214)	H-acceptor	2.79
		propanolol	-34.4	N(11)-NE2.HIS(199)	H-donor	2.78
		phenytoin	-10.0	N(19-NE2.HIS(199)	H-donor	3.04
MAPK3	4QTB	F5	-9.3	O(36)-NZ_LYS(71)	H-acceptor	2.96
		F9	-10.1	O(49)-NZ_LYS(71)	H-acceptor	2.93
		M1	-8.3	O(39)-NZ_LYS(71)	H-acceptor	2.9
		P1	-6.0	O(22)-NZ_LYS(71)	H-acceptor	2.9
		P3	-14.5	O(39)-NZ_LYS(71)	H-acceptor	2.84
		P10	-11.2	O(27)-NZ_LYS(71)	H-acceptor	2.86
		P11	-11.6	O(27)-NZ_LYS(71)	H-acceptor	2.96
		P14	-6.4	O(23)-NZ_LYS(71)	H-acceptor	2.91
		P24	-15.2	O(15)-NZ_LYS(71)	H-acceptor	2.88
		P29	-13.7	O(21)-NZ_LYS(71)	H-acceptor	2.81
		P31	-5.2	O(19)-NZ_LYS(71)	Ionic	2.89
		P39	-8.4	O(20)-NZ_LYS(71)	H-acceptor	2.93
		P41	-5.4	O(23)-NZ_LYS(71)	Ionic	287
		P42	-13.6	O(16)-NZ_LYS(71)	H-acceptor	2.86
		P43	-6.1	O(22)-NZ_LYS (71)	H-acceptor	2.88
		P45	-5.1	O(41)-NZ_LYS(71)	H-acceptor	2.76
		P53	-7.3	O(38)-NZ_LYS(71)	H-acceptor	3.01
		P54	-9.6	O(17)-NZ_LYS(71)	H-acceptor	2.86
		sitagliptin	-13.8	N)41)-NZ_LYS(71)	H-acceptor	2.8

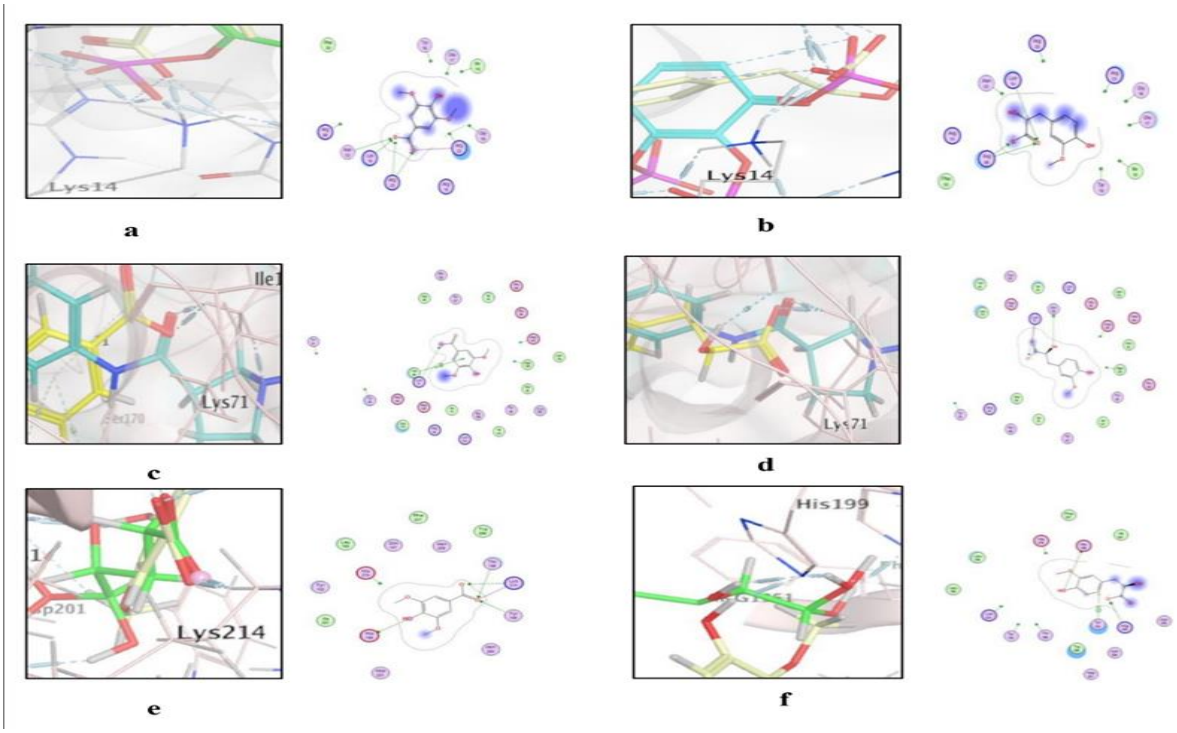

Figure 4. Molecular docking interactions between HL compounds and target proteins. Docking analysis revealed eight strong interactions between two HL bioactive compounds, P41 (syringic acid) and P43 (vanillactic acid), and three key protein targets: (a) AKT1-P41, (b) AKT1-P43, (c) MAPK3-P41, (d) MAPK3-P43, (e) HIF1A-P41, (f) HIF1A-P43. AKT1: Serine/threonine kinase 1; MAPK3: Mitogen-activated protein kinase 3; HIF1A: hypoxia-inducible factor 1-alpha.

HaCaT cell proliferation assay

HL extract and lobeline were tested on HaCaT cells at concentrations of 62.5 to 0.97 ppm. HL significantly enhanced cell proliferation at all concentrations ($p<0.0001$), with the strongest effect observed at 15.62 ppm (Figure 5A) compared to the negative control (NC = 0.125% DMSO in medium). In contrast, lobeline significantly increased proliferation only at 1.95 ppm ($p<0.01$) (Figure 5B). The DMSO-only group showed no cytotoxicity, confirming that the observed effects were due to the test compounds. Based on the results, the concentrations selected for subsequent assay were HL 31.25 (K1), 15.62 (K2), and 7.81 ppm (K3); and lobeline 3.90 (L1), 1.95 (L2), and 0.98 ppm (L3). These findings indicate that the tested concentrations are non-toxic and promote HaCaT cell proliferation.

TNF-α level by ELISA

Among all HL-treated groups, only K1 (31.25 ppm) significantly reduced TNF-α level in comparison to the high-glucose (HG) group ($p < 0.05$) (Figure 6A). The absence of a clear dose-dependent effect may be due to variation in the concentrations of active constituents within the crude extract.

Histopathological analysis of inflammatory cells

No indications of toxicity, aberrant behavior, or mortality were detected in the animals treated with HL extract, indicating good tolerability of the tested doses. H&E staining revealed a time-dependent reduction in inflammatory cells from day 7 to 21. By day 14, all HL-treated groups (30%, 40%, and 50%) showed significantly fewer inflammatory cells than the base control ($p < 0.01$), while only the 50% group maintained this significance on day 21 ($p < 0.05$) (Figure 6B and 6C). These findings support the anti-inflammatory effects of HL in diabetic wound healing, consistent with the *in vitro* results.

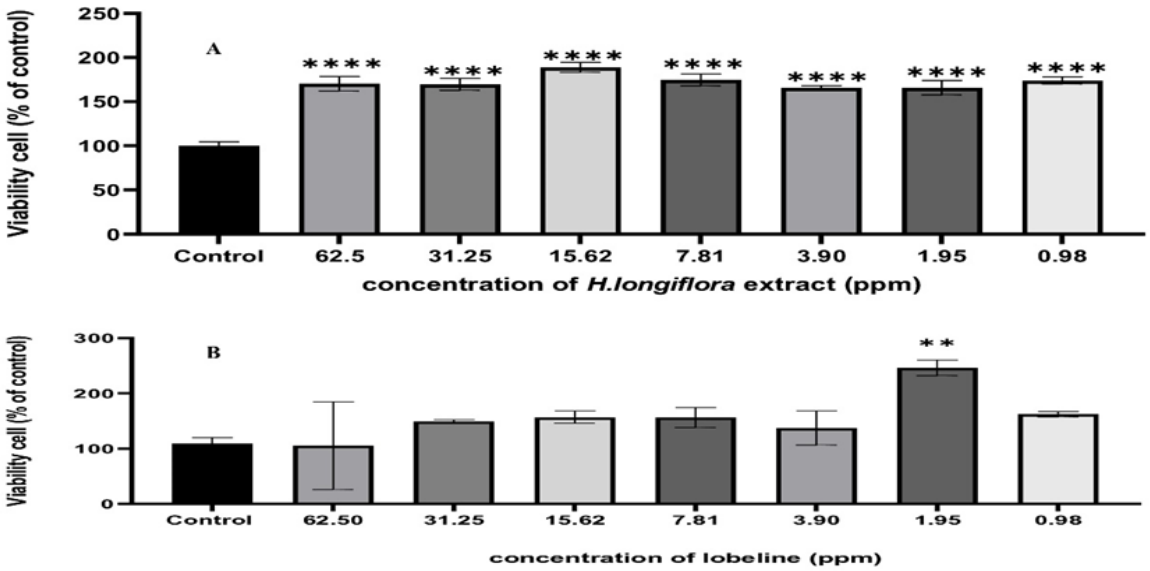

Figure 5. Viability of HaCaT cells treated with *Hippobroma longiflora* (HL) extract and lobeline. (A) shows that all tested concentrations of HL significantly increased HaCaT cell viability compared to the control (****p<0.0001); 31.25, 15.62, and 7.81 ppm were selected for further analysis. (B) indicates that 1.95 ppm of lobeline significantly increased cell viability (**p<0.01). Additional comparisons were made using lobeline at 3.90 ppm and 0.98 ppm alongside HL. Control cell: 0.125% DMS

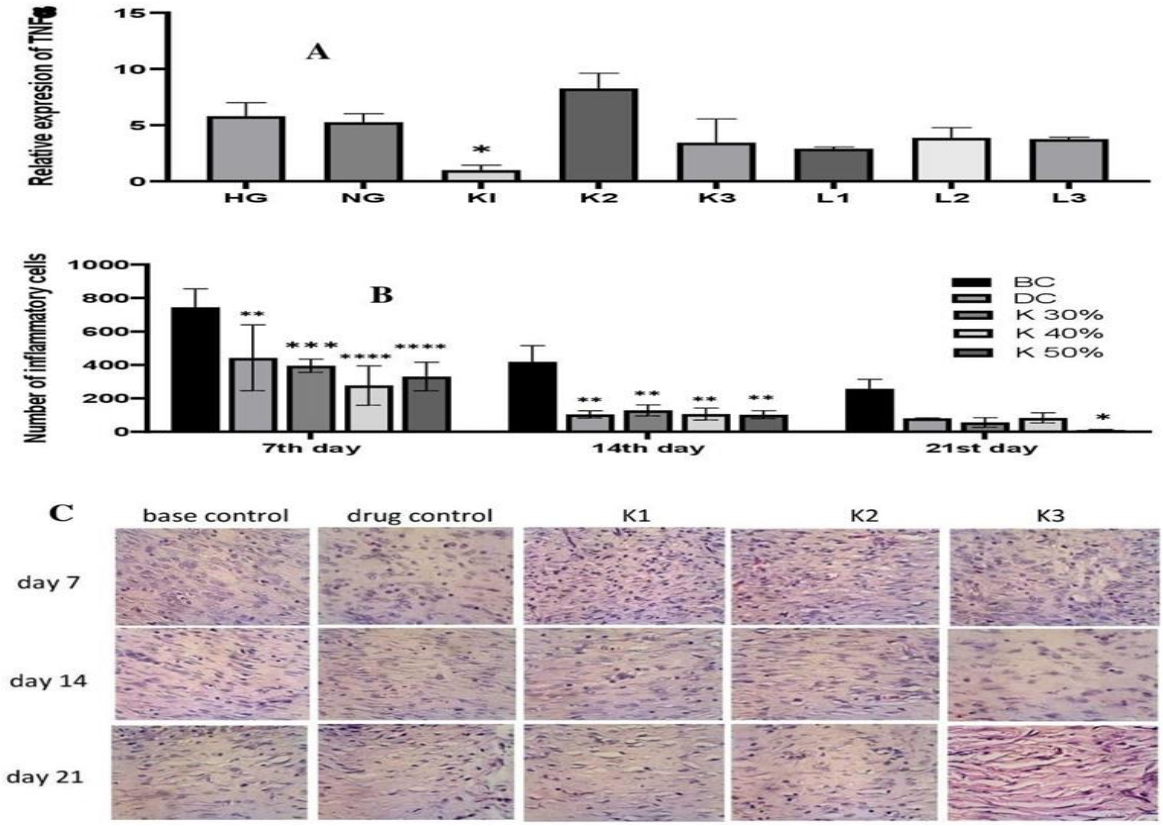

Figure 6. Anti-inflammatory effects of *Hippobroma longiflora* (HL) in *in vitro* and *in vivo* studies. (A) shows the relative expression of TNF-α measured by ELISA. The K1 group (31.25 ppm HL) showed a significant reduction compared to the high glucose (HG) group (*p<0.05). HG: high glucose (9008 ppm = 50 mM); NG: normo glucose (900,8 ppm = 5 mM); K1-K3: HL extract (31.25, 15.62, and 7.81 ppm); L1-L3: lobeline (3.90, 1.95, and 0.98 ppm). (B) displays the inflammatory cell count over time. On day 7, the treatment group showed a greater reduction than the drug control (DC), with ****p<0.0001 vs. base control (BC) and **p<0.01 for DC vs. BC. On day 14, both treatment and DC groups differed significantly from BC (**p<0.01). on day 21, only the K50% group showed a significant difference compared to BC (p<0.05). (C) presents histological images showing inflammatory cell presence at various time points. Dark-stained dots represent inflammatory cells. BC: base control; DC: drug control; K30-50%: HL extract at (K1) 30%, (K2) 40%, and (K3) 50%.

Discussion

Natural products, particularly phenolics and alkaloids, are increasingly recognized as promising agents for chronic wound management, including diabetic ulcers (Accipe et al. 2023). Flavonoids are recognized for their antioxidant and anti-inflammatory characteristics (Ginwala et al. 2019), while alkaloids exhibit antimicrobial and antiviral effects (Abass et al. 2024). This study examined the wound-healing efficacy of HL leaf extract using a comprehensive methodology that included phytochemical profiling, network pharmacology, molecular docking, and experimental validation.

LC-HRMS analysis confirmed the presence of both known and potentially novel bioactive metabolites in HL extract, including syringic acid, vanillactic acid, and lobeline. This technique, known for its high sensitivity in complex herbal matrices (Aydoğan 2020; Stock 2017), provided a basis for further *in silico* prediction and target analysis.

SwissTargetPrediction indicated multiple protein targets, which were further validated through molecular docking. Notably, syringic acid and vanillactic acid exhibited strong binding to three key proteins: AKT1, MAPK3, and HIF-1α, implicated in proliferation, angiogenesis, and tissue regeneration. Compared to conventional drugs, HL-derived phenolics displayed broader protein interactions, suggesting multi-target therapeutic potential. Although docking scores were slightly lower than those of standard drugs, their ability to engage multiple wound-related targets confers a distinct pharmacological advantage.

GO and KEGG enrichment analyses further supported HL therapeutic relevance. Key biological processes included gene expression regulation, lipopolysaccharide (LPS) signaling, and angiogenesis, while enriched pathways involved HIF-1 signaling and lipid metabolism. Despite some enrichment in cancer-related pathways, likely due to overlapping molecular cascades, the central role of HIF-1α in diabetic wound healing underscores the importance of this target (Rai et al. 2022).

Chronic diabetic wounds are driven by sustained inflammation, marked by elevated IL-1β and TNF-α levels (Dasari et al. 2021; Spampinato et al. 2020). *In vitro*, HL significantly reduced TNF-α expression at 31.25 ppm (K1), supporting its concentration-dependent anti-inflammatory activity. Lobeline alone did not show similar effects, suggesting that other constituents, particularly syringic acid, may be responsible. *In vivo*, reduced inflammatory cell infiltration by day 21 indicated a possible shift from M1 to M2 macrophage polarization (Aitcheson et al. 2021), a key step in resolving inflammation and initiating repair.

Syringic acid has been shown to inhibit NF-κB, IL-1β, TNF-α, and IL-2, while promoting antioxidant activity and epithelial regeneration (Chen et al. 2023; Ren et al. 2019). Though vanillactic acid remains understudied, its structural similarity to vanillic acid and strong docking scores suggest comparable anti-inflammatory potential. These findings warrant further investigation of vanillactic acid as a potential novel therapeutic candidate.

Collectively, the reduction in TNF-α levels and inflammatory cells aligns with the molecular docking predictions of HL-derived compounds targeting key regulators such as AKT1, MAPK3, and HIF-1α. These proteins play essential roles in keratinocyte proliferation, angiogenesis, and wound re-epithelialization, providing mechanistic insight into the wound-healing effects of HL extract.

Importantly, topical HL application on rats did not cause toxicity, behavioral changes, or skin irritation, despite the known systemic toxicity of its alkaloids (e.g., lobeline and nicotine). These findings suggest that dermal exposure at the tested doses is well tolerated. Nevertheless,

comprehensive toxicological profiling is needed for clinical translation.

From a translational standpoint, HL extract offers a promising multi-target, dual-action (anti-inflammatory and pro-proliferative) therapeutic candidate for diabetic wounds, particularly valuable in resource-limited settings. The combined use of phytochemical, computational, and *in vivo* data strengthens the translational relevance of this study.

This study has several limitations. First, the *in vivo* sample size was limited (n = 3 per subgroup), reducing statistical power. Second, inflammatory cell analysis relied on H&E staining without immunohistochemical or molecular confirmation. Third, while docking and network pharmacology provided mechanistic predictions, they require further validation through biochemical assays. Lastly, only a subset of HRMS-identified compounds was evaluated, potentially overlooking other active constituents.

Future work should focus on dose–response studies, immunohistochemical validation (e.g., for TNF-α, IL-1β, and Vascular Endothelial Growth Factor (VEGF), compound isolation, pharmacokinetic profiling, and comprehensive safety evaluations to support potential clinical

This study employs an integrative methodology that combines network pharmacology, molecular docking, and experimental validation to highlight the multi-target therapeutic potential of *H. longiflora* (HL) in diabetic wound healing. HL exerted dual effects by attenuating inflammation through the modulation of IL-1β and TNF-α, and enhancing proliferation via the AKT1, MAPK3, and HIF-1α signaling pathways. Syringic acid and vanillactic acid were identified as key bioactive compounds mediating these effects. By targeting multiple phases of wound healing, HL presents a promising, affordable, and accessible therapeutic option, particularly in settings where conventional treatments are limited.

Acknowledgment

The author thanks the Indonesian Education Scholarship in 2022, which provided funding with the master number 202209092924; the Center for Higher Education Funding and Assessment, Ministry of Higher Education, Science and Technology of the Republic of Indonesia; Indonesia Endowment Fund for Education supported this work.

Conflicts of interest

The authors declare no conflicts of interest relevant to this study.

Funding

The Indonesian Education Scholarship in 2022, which provided funding with the master number 202209092924; Center for Higher Education Funding and Assessment, Ministry of Higher Education, Science and Technology of the Republic of Indonesia; Indonesia Endowment Fund for Education supported this work.

Ethical considerations

All animal experiments were conducted by institutional and national guidelines for the care and use of laboratory animals and approved by the Ethical Clearance Committee of the Faculty of Medicine, Public Health, and Nursing, Universitas Gadjah Mada, Yogyakarta, Indonesia, under ethical approval number KE/FK/1490/EC/2023.

Code of ethics

This manuscript complies with the principles of publication ethics. The authors confirm that the work is original, contains no plagiarism or data manipulation, and has not been submitted elsewhere. All authors have approved the final version and agree with its submission.

Authors' contributions

Conceptualization: ZI, HEM; Methodology: RM, HEM: Software: HEM, NF, HH; Validation: ZI, RM, NF; Formal Analysis: NF; Investigation: HEM; Resource: ZI, RM, NF, HEM, Data Curation: HEM, Project Administration: ZL, HEM; Visualization: RM, HEM; Supervision: ZI, RM, NF; Writing – Original draft: HEM; Writing- Review & Editing: ZI, RM, NF, HH, HEM.

References

Abass S, Parveen R, Irfan M, Malik Z, Husain SA, Ahmad S (2024) Mechanism of antibacterial phytoconstituents: an updated review. Arch Microbiol 206(7):1-21 doi:10.1007/s00203-024-04035-y

Accipe L, Abadie A, Neviere R, Bercion S (2023) Antioxidant Activities of Natural Compounds from Caribbean Plants to Enhance Diabetic Wound Healing. Antioxidants 12(5):1-28 doi:10.3390/antiox12051079

Ahda M, Jaswir I, Khatib A, et al. (2023) Phytochemical analysis, antioxidant, α-glucosidase inhibitory activity, and toxicity evaluation of Orthosiphon stamineus leaf extract. Sci Rep 13(1):1-11 doi:10.1038/s41598-023-43251-2

Aitcheson SM, Frentiu FD, Hurn SE, Edwards K, Murray RZ (2021) Skin wound healing: Normal macrophage function and macrophage dysfunction in diabetic wounds. Molecules 26(16):1-11 doi:10.3390/molecules26164917

Amrati FEZ, Chebaibi M, Galvão de Azevedo R, et al. (2023) Phenolic Composition, Wound Healing, Antinociceptive, and Anticancer Effects of Caralluma europaea Extracts. Molecules 28(4) doi:10.3390/molecules28041780

Aydoğan C (2020) Recent advances and applications in LC-HRMS for food and plant natural products: a critical review. Anal Bioanal Chem 412(9):1973-1991 doi:10.1007/s00216-019-02328-6

Burgess JL, Wyant WA, Abujamra BA, Kirsner RS, Jozic I (2021) Diabetic Wound-Healing Science. Medicina 57(1072):1-24 doi:10.3390/medicina57101072

Chanu NR, Gogoi P, Barbhuiya PA, Dutta PP, Pathak MP, Sen S (2023) Natural Flavonoids as Potential Therapeutics in the Management of Diabetic Wound: A Review. Curr Top Med Chem 23(8):690-710 doi:10.2174/1568026623666230419102140

Chen J, Qin S, Liu S, et al. (2023) Targeting matrix metalloproteases in diabetic wound healing. Front Immunol 14(February):1-19 doi:10.3389/fimmu.2023.1089001

Chumpolphant S, Suwatronnakorn M, Issaravanich S, Tencomnao T, Prasansuklab A (2022) Polyherbal formulation exerts wound healing, anti-inflammatory, angiogenic and antimicrobial properties: Potential role in the treatment of diabetic foot ulcers. Saudi J Biol Sci 29(7):103330-103330 doi:10.1016/j.sjbs.2022.103330

Dasari N, Jiang A, Skochdopole A, et al. (2021) Updates in Diabetic Wound Healing, Inflammation, and Scarring. Semin Plast Surg 35(3):153-158 doi:10.1055/s-0041-1731460

Davis FM, Kimball A, Boniakowski A, Gallagher K (2018) Dysfunctional Wound Healing in Diabetic Foot Ulcers: New Crossroads. Curr Diab Rep 18(1) doi:10.1007/s11892-018-0970-z

den Dekker AD, Davis FM, Joshi AD, et al. (2020) TNF-α regulates diabetic macrophage function through the histone acetyltransferase MOF. JCI Insight 5(5):1-13 doi:10.1172/jci.insight.132306

Deng H, Li B, Shen Q, et al. (2023) Mechanisms of diabetic foot ulceration : A review. J Diabetes 15(February):299-312 doi:10.1111/1753-0407.13372

Dong MW, Li M, Chen J, et al. (2016) Activation of α7nAChR Promotes Diabetic Wound Healing by Suppressing AGE-Induced TNF-α Production. Inflammation 39(2):687-699 doi:10.1007/s10753-015-0295-x

Falanga V (2005) Wound healing and its impairment in the diabetic foot. Lancet 366(9498):1736-1743 doi:10.1016/S0140-6736(05)67700-8

Fu S, Zhou Y, Hu C, Xu Z, Hou J (2022) Network pharmacology and molecular docking technology-based predictive study of the active ingredients and potential targets of rhubarb for the treatment of

diabetic nephropathy. BMC Complement MedTher 22(1):1-20 doi:10.1186/s12906-022-03662-6

Furman BL (2021) Streptozotocin-Induced Diabetic Models in Mice and Rats. Current Protocol 1:1-21 doi:10.1002/cpz1.78

Ginwala R, Bhavsar R, Chigbu DGI, Jain P, Khan ZK (2019) Potential Role of Flavonoids in Treating Chronic Inflammatory Diseases with a Special Focus on the Anti-Inflammatory Activity of Apigenin. antioxidan 8(2):1-28 doi:10.3390/antiox8020035

Heyne K (1987) Tumbuhan berguna Indonesia I, vol III,

Kesting JR, Tolderlund IL, Pedersen AF, Witt M, Jaroszewski JW, Staerk D (2009) Piperidine and tetrahydropyridine alkaloids from Lobelia siphilitica and Hippobroma longiflora. J Nat Prod 72(2):312-315 doi:10.1021/np800743w

Liu Y, Liu Y, Deng J, Li W, Nie X (2021) Fibroblast Growth Factor in Diabetic Foot Ulcer: Progress and Therapeutic Prospects. Front Endocrinol (Lausanne) 12(October):1-14 doi:10.3389/fendo.2021.744868

Murdiana HE, Murwanti R, Fakhrudin N, Ikawati Z (2024) Multi-target mechanism of polyherbal extract to treat diabetic foot ulcer based on network pharmacology and molecular docking. J HerbMed Pharmacol 13(2):289-299 doi:10.34172/jhp.2024.49362

Qaseem A, Barry MJ, Humphrey LL, et al. (2017) Oral pharmacologic treatment of type 2 diabetes mellitus: A clinical practice guideline update from the American college of physicians. Ann Intern Med 166(4):1-20 doi:10.7326/M16-1860

Rai V, Moellmer R, Agrawal DK (2022) Enhancing Chronic Diabetic Foot Ulcer Healing. Cell 11(2287):1-14 doi:10.3390/cells11152287

Raja JM, Maturana MA, Kayali S, Khouzam A, Efeovbokhan N (2023) Diabetic foot ulcer: A comprehensive review of pathophysiology and management modalities. World J Clin Cases 11(8):1684-1693 doi:10.12998/wjcc.v11.i8.1684

Ren J, Yang M, Xu F, Chen J, Ma S (2019) Acceleration of wound healing activity with syringic acid in streptozotocin induced diabetic rats. Life Sci 233(August):116728-116728 doi:10.1016/j.lfs.2019.116728

Růžička J, Dejmek J, Bolek L, Beneš J, Kuncová J (2021) Hyperbaric Oxygen Influences Chronic Wound Healing – a Cellular Level Review. Physiol Res 70(Jain 2009):261-273 doi:10.33549/physiolres.934822

Spampinato SF, Caruso GI, Pasquale RD, Sortino MA, Merlo S (2020) The Treatment of Impaired Wound Healing in Diabetes : Looking among Old Drug. pharmaceutical 13(60):1-17 doi:10.3390/ph13040060

Stock NL (2017) Introducing Graduate Students to High-Resolution Mass Spectrometry (HRMS) Using a Hands-On Approach. J Chem Educ 94(12):1978-1982 doi:10.1021/acs.jchemed.7b00569

Suryavanshi SV, Kulkarni YA (2017) NF-κβ: A potential target in the management of vascular complications of diabetes. Front Pharmacol 8(NOV):1-12 doi:10.3389/fphar.2017.00798

Wang X, Jiang G, Zong J, et al. (2022) Revealing the novel ferroptosis-related therapeutic targets for diabetic foot ulcer based on the machine learning. Front Genet 13(September):1-14 doi:10.3389/fgene.2022.944425

WHO (2016) Global Report on Diabetes. vol 978. World Health Organization p11-11

Zheng S-Y, Wan X-X, Kambey PA, et al. (2023) Therapeutic role of growth factors in treating diabetic wound. World J Diabetes 14(4):364-395 doi:10.4239/wjd.v14.i4.364